Clinical implications of intraoperative infrared brain surface monitoring during superficial temporal artery–middle cerebral artery anastomosis in patients with moyamoya disease

Clinical article

ATSUHIRO NAKAGAWA, M.D., PH.D.,[1] MIKI FUJIMURA, M.D., PH.D.,[1]
TATSUHIKO ARAFUNE, PH.D.,[2] ICHIRO SAKUMA, PH.D.,[2] AND TEIJI TOMINAGA, M.D., PH.D.[1]

[1]Department of Neurosurgery, Tohoku University Graduate School of Medicine, Sendai, Miyagi;
and [2]Bio-Medical Precision Engineering Laboratory, Institute of Environmental Studies, Graduate
School of Frontier Sciences, The University of Tokyo, Japan

Object. Surgical revascularization for moyamoya disease prevents cerebral ischemic attacks by improving cerebral blood flow (CBF). Symptomatic cerebral hyperperfusion is a potential complication of this procedure, but its treatment is contradictory to that for ischemia. Because intraoperative techniques to detect hyperperfusion are still lacking, the authors performed intraoperative infrared monitoring in moyamoya disease using a novel infrared imaging system.

Methods. During superficial temporal artery–middle cerebral artery anastomosis in 25 patients (26 hemispheres) with moyamoya disease, the authors monitored the brain surface temperature intraoperatively with the IRIS-V infrared imaging system. The average gradation value change (indicating temperature change) was calculated using commercial software. Magnetic resonance imaging, MR angiography, and *N*-isopropyl-*p*-[^{123}I]iodoamphetamine SPECT studies were performed routinely before and within 10 days after surgery.

Results. Patency of bypass, detailed local hemodynamics, and changes in cortical surface temperature around the anastomosis site were well recognized by the IRIS-V infrared imaging system in all cases. In the present study, 10 patients suffered transient neurological symptoms accompanied by an increase in CBF around the anastomosis site, recognized as symptomatic hyperperfusion. The increase in temperature was significantly higher in these patients. Intensive blood pressure control was undertaken, and free-radical scavengers were administered. No patient in the present study suffered a permanent neurological deficit.

Conclusions. Although the present method does not directly monitor surface CBF, temperature rise around the anastomosis site during surgery might be an indicator of postoperative hyperperfusion. Prospective evaluation with a larger number of patients is necessary to validate this technique. *(DOI: 10.3171/2009.4.JNS08585)*

KEY WORDS • extracranial-intracranial bypass • thermal artery imaging • intraoperative monitoring • minimally invasive neurosurgery • neurocritical care

MOYAMOYA disease is a chronic, occlusive cerebrovascular disease with unknown etiology and is characterized by bilateral stenoocclusive changes at the terminal portion of the internal carotid artery and an abnormal vascular network at the base of the brain.[22] Surgical revascularization for moyamoya disease is believed to be beneficial to prevent cerebral ischemic attacks by improving CBF, and STA-MCA anastomosis with or without indirect bypass is generally used as the standard surgical treatment.[11,12] On the other hand, several lines of evidence support that not only ischemia but symptomatic cerebral hyperperfusion is a potential complication of this procedure in the acute stage.[5–8,16] Accurate and early diagnosis of postoperative hyperperfusion is important because its treatment is contradictory to that for ischemia. Because intraoperative techniques to estimate subsequent occurrence of symptomatic hyperperfusion are still lacking, we performed intraoperative infrared monitoring of the surface brain temperature by using a novel infrared imaging system in the hope that we can indirectly evaluate changes in surface CBF. We also evaluated the clinical impact of temperature change on occurrence of symptomatic hyperperfusion during the acute stage after revascularization.

Abbreviations used in this paper: CBF = cerebral blood flow; DW = diffusion weighted; EDMS = encephaloduromyosynangiosis; ^{123}I-IMP = *N*-isopropyl-*p*-[^{123}I]iodoamphetamine; MCA = middle cerebral artery; ROI = region of interest; STA = superficial temporal artery; TIA = transient ischemic attack.

Methods

Between March 2005 and December 2006 at Tohoku University Hospital, we conducted intraoperative monitoring of brain surface blood flow by using the IRIS-V infrared imaging system (Sparkling Photon, Inc.) during STA-MCA anastomosis on 26 hemispheres in 25 patients with moyamoya disease (female/male ratio 16:9; age range 7–63 years, mean age 33.4 years). All patients met the criteria of the Research Committee on Spontaneous Occlusion of the Circle of Willis, of the Ministry of Health, Labor, and Welfare, Japan. Standard angiography was performed preoperatively in all adult patients and whenever possible in pediatric patients. All patients underwent STA-MCA anastomosis consisting of EDMS and dural pedicle insertion.[20] During surgery the patients were kept normotensive with normocapnia and a rectal temperature of 36°C. The room temperature was maintained at 23°C to keep the background cortical surface temperature as constant as possible. After completion of anastomosis, the high-resolution infrared camera of the IRIS-V infrared imaging system was set 30 cm above the brain, and blood flow was continuously monitored for as long as 3 minutes, including time for placement and release of the temporary clip (Fig. 1). We used this method instead of monitoring before and after the surgical procedure because the cortical temperature before starting the surgical procedure would have been recorded long before completion of the bypass procedure, and thus might not have been as accurate as the baseline value because of temperature changes from the time of craniotomy until the end of the bypass procedure.[17]

The IRIS-V infrared imaging system is composed of 3 parts: a main computer, a camera head, and a display monitor. The size of the camera head is $14 \times 16 \times 19$ cm. The camera is connected to the main computer part by folded 5-joint arms (maximum horizontal distance: 80 cm, possible vertical motorized distance 125–155 cm above floor) so that surgeons can bring the camera head over the operative field whenever necessary. The infrared focal plane array detector (barium strontium titanate, 320×240 pixels) shows an area of 110×82 mm using an F50 infrared lens. The detectable temperature is limited to $35 \pm 10°C$. Temperatures $> 45°C$ are shown in black, whereas those $< 25°C$ are shown in white and are presented as 8-bit black-and-white images in each pixel. The detectable wavelength band is 7–14 μm. No contrast medium or radiation was used to obtain the images. The recording speed was 30 frames/second. All of the images were stored in the installed computer and recorded with a digital video device. Obtained images were analyzed with imaging software by changes in gradation value.[13,17,24] In addition, the ROI was set around the anastomosis site (diameter 100 pixels), and the average gradation value within the ROI was calculated by Matrox Inspector software (version 8.0, Matrox Electronics Systems, Ltd.). Probability values < 0.05 were considered to be statistically significant.

In all cases, preoperative CBF was measured using ^{123}I-IMP-SPECT. The ^{123}I-IMP-SPECT studies were routinely performed before surgery and 1 and 7 days after surgery in all cases. Before surgery and within 10 days of surgery, 1.5-T MR imaging and MR angiography were routinely performed. Standard angiography was not performed postoperatively.[6] The MR imaging studies included DW images, FLAIR images, T1- and T2-weighted images, and T2*-weighted images.

Results

Patency of bypass could be evaluated in all cases attempted, and it was also confirmed by conventional Doppler ultrasonography during the operation and by postoperative MR angiography during the follow-up period. Information regarding local hemodynamics, which includes flow direction and distribution, could also be evaluated in all cases by the IRIS-V infrared imaging system throughout the craniotomy. Among the 25 patients who underwent 26 surgeries, 10 suffered transient postoperative neurological deterioration. These patients exhibited an intense increase in CBF around the anastomosis site as detected by ^{123}I-IMP-SPECT and a thick STA on MR angiography.[5-7] Intensive blood pressure control with administration of oxygen radical scavengers was performed, and no patient suffered permanent neurological deterioration compared with his or her preoperative neurological status. Transient ischemic attacks disappeared or improved in all cases during the follow-up period.

Representative Cases

Case 1

Presentation. This 54-year-old man presented with frequent TIAs (transient weakness in the left extremity). Stage III moyamoya disease was identified, and ^{123}I-IMP-SPECT showed that his right CBF and cerebrovascular reserve capacities were markedly impaired. Therefore, STA-MCA anastomosis with EDMS was performed in the right hemisphere.

Operation. After exploration of the parietal branch of the right STA, a frontotemporoparietal craniotomy was performed. The recipient artery at the M_4 segment of the anterior parietal branch of the MCA was explored, and anastomosis was performed between the stump of the STA (2.0 mm in diameter) and the M_4 segment (1.0 mm in diameter). Then, EDMS and dural pedicle insertion were performed. Intraoperative infrared monitoring disclosed changes in the color of the bypass to white after the temporary occlusion (indicating decrease in temperature) (Fig. 2 *upper left*), and then a change to black (indicating increase in temperature) 2 seconds after removal of the clip (Fig. 2 *lower left*), indicating presence of blood flow and patency of the bypass. During the color change, the cooled blood was shown to be pushed away toward the cranial artery, in both proximal and distal directions of the M_4 segment at 1.00 second (Fig. 2 *upper right*), indicating the presence of a perfusion pressure gradient (Fig. 2 *upper right*). The patency of the bypass was also confirmed by intraoperative Doppler ultrasonography. The color of the exposed brain around the anastomosis site did
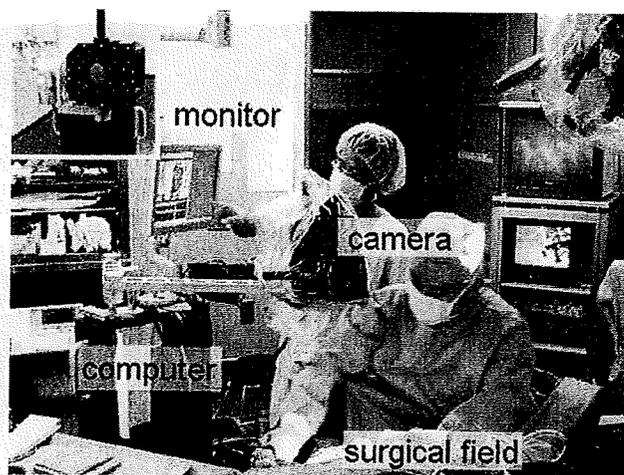
Fig. 1. Photograph of the IRIS-V infrared imaging system in the operating theater. *Inset:* The infrared and charge-coupled device camera.
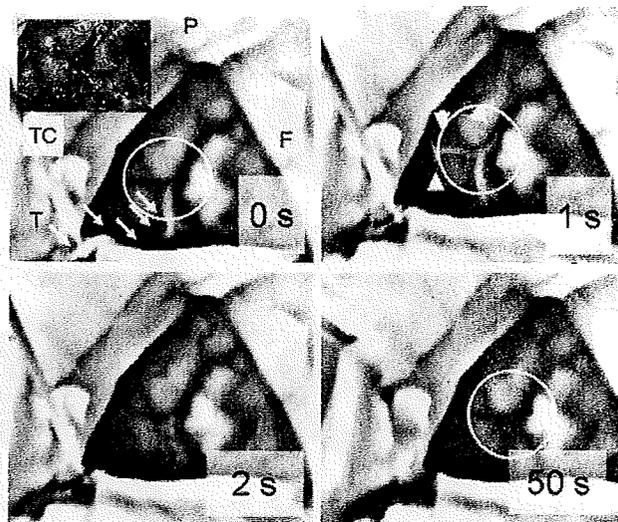

Fig. 2. Case 1. Microscopic views of the surgical field around the anastomosis *(inset, upper left)* and intraoperative infrared monitoring showing changes in color of the STA *(arrows)* to white after temporary occlusion, indicating decrease in temperature *(upper left)* due to the absence of blood flow. Right after removal of the clip at 1 second, the color of the bypass transiently changed to white by cooled blood flow *(upper right, arrowheads)* and then changed to black (indicating an increase in temperature) at 2 seconds *(lower left),* indicating patency of the bypass. Note that the brain surface color around the anastomosis site *(circle, lower right)* did not significantly change throughout the process. F = frontal lobe; P = parietal lobe; T = temporal lobe; TC = temporary clip.

not show significant change before and after removal of the temporary clip (Fig. 2). The change in average gradation value within the ROI was within 5 points, indicating no significant increase in temperature after release of the temporary clip (Fig. 3).

Postoperative Course. The patient's postoperative course was uneventful. Patency of the bypass was also confirmed by MR angiography. The ^{123}I-IMP-SPECT studies performed 1 and 7 days after surgery showed a slight increase in CBF in the right hemisphere compared with the preoperative findings. Postoperative DW MR imaging showed no evidence of ischemic change, and MR angiography demonstrated the apparently patent STA-MCA bypass as a higher intensity signal than the opposite side STA. The patient did not experience neurological deterioration during the follow-up period.

Case 2

Presentation. This 26-year-old woman presented with a TIA (transient weakness in the left upper extremity). Stage III moyamoya disease was identified, and ^{123}I-IMP-SPECT showed that her bilateral CBF and cerebrovascular reserve capacities were markedly impaired. Therefore, bilateral bypass surgery was planned.

Operation. An STA-MCA anastomosis with EDMS was performed in the right hemisphere. After exploration of the parietal branch of the right STA, a frontotemporoparietal craniotomy was performed. The recipient artery at the M_4 segment of the anterior parietal branch of the MCA was explored, and anastomosis was performed between the stump of the STA (1.0 mm in diameter) and the M_4 segment (0.8 mm in diameter). Then an EDMS procedure and dural pedicle insertion were performed. Intraoperative infrared monitoring disclosed changes in the color of the bypass to white after the temporary occlusion (indicating a decrease in temperature) (Fig. 4 *upper left*), and a change to black (indicating an increase in temperature) after removal of the clip, indicating presence of

blood flow and patency of the bypass (Fig. 4 *upper right* and *lower left*). Patency of the bypass was also confirmed by intraoperative Doppler ultrasonography. The images also disclosed that the color of the brain surface around the anastomosis changed significantly to black after removal of the temporary clip until the end of monitoring (Fig. 4 *lower right*). The change of average gradation value within the ROI increased 15–20 points, indicating a significant increase of temperature after release of the temporary clip (Fig. 5).

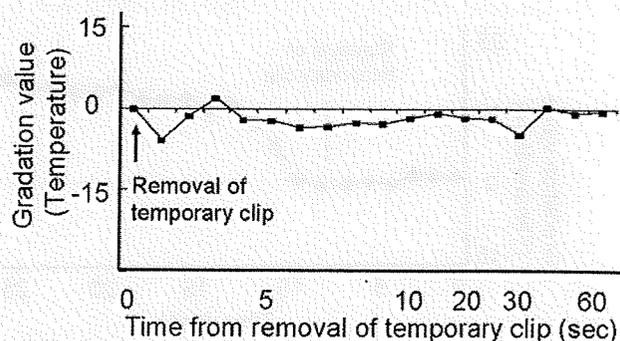*Operation.* The patient showed no evidence of neu-

Fig. 3. Graph showing the relationship between time after removal of the temporary clip and changes of the average gradation value within the ROI around the anastomosis site as evaluated using imaging software in Case 1. The increase of gradation value after removal of the temporary clip was within 5 points, indicating no significant change in surface temperature.
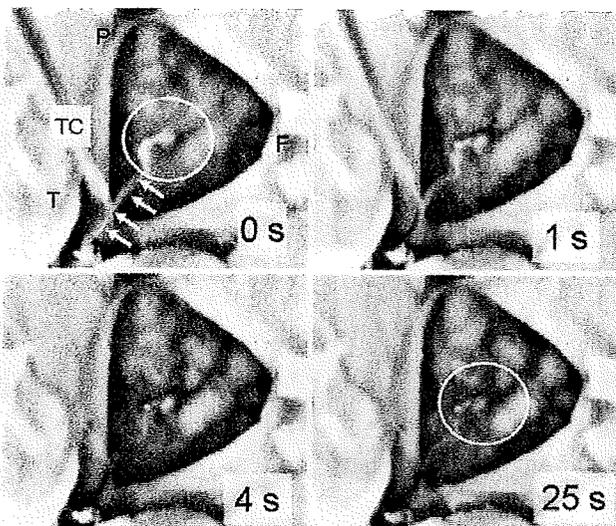
FIG. 4. Case 2. Images obtained during intraoperative infrared monitoring disclosing changes in color in the color in the STA (arrows) to white after temporary occlusion (indicating decrease in temperature; upper left) due to the absence of blood flow. Immediately after removal of clip at 1 second, the color of the bypass changes to black (upper right), indicating the presence of blood flow. The area is even darker after 4 seconds (lower left). Note that the color of the brain surface around the anastomosis site (circle, lower right) gradually changes to black (indicating an increase in temperature).

rological deficit immediately after surgery. The ^{123}I-IMP-SPECT studies obtained 1 day after surgery showed a slight increase in CBF in the right hemisphere (Fig. 6 center) compared with the preoperative findings (Fig. 6 upper). Postoperative DW MR imaging showed no evidence of ischemic change, and MR angiography demonstrated the apparently patent STA-MCA bypass as a higher intensity signal than the contralateral STA (Fig. 7 arrowhead). One day later, she suffered from fluctuating dysarthria, left facial palsy, and numbness in the left upper limb. A ^{123}I-IMP-SPECT study showed a focal intense increase in CBF at the site of anastomosis 7 days after surgery (Fig. 7 lower). A diagnosis of hyperperfusion was thus made based on neurological symptoms along with ^{123}I-IMP

FIG. 6. The ^{123}I-IMP-SPECT studies obtained preoperatively (upper), 1 day after surgery (center) and 8 days after surgery (lower). Note the focal intense increase in the CBF at the site of anastomosis (arrowheads in lower).

SPECT and MR angiography findings. Intensive blood pressure control and the use of a free radical scavenger relieved her symptoms, which completely disappeared 13 days after surgery, at which time she was discharged from the hospital without neurological deficit. We performed second-stage surgery on the left side 1 month later.

Postoperative Course. She was discharged uneventfully after successful left STA-MCA anastomosis and EDMS, which resulted in disappearance of her ischemic attacks as well as a significant improvement in CBF on the bilateral cerebral hemisphere. She did not exhibit neurological deterioration during the follow-up period.

Neurological Deterioration

In all, 10 patients suffered from transient postoperative neurological deterioration, which were proved to be due to hyperperfusion in the present series. The aver-
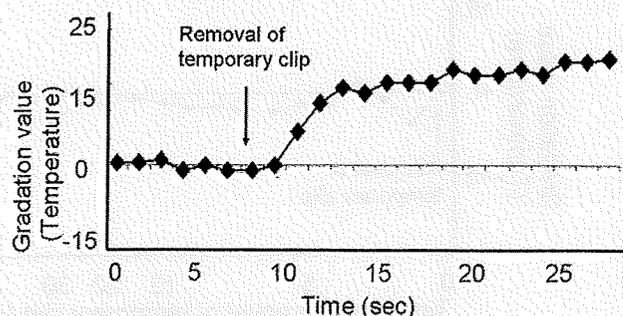
FIG. 5. Graph showing the relationship between time after removal of the temporary clip and changes in average gradation value within the ROI around the anastomosis site as evaluated by imaging software in Case 2. There was a significant rise of gradation value after removal of the temporary clip, indicating significant change in surface temperature.
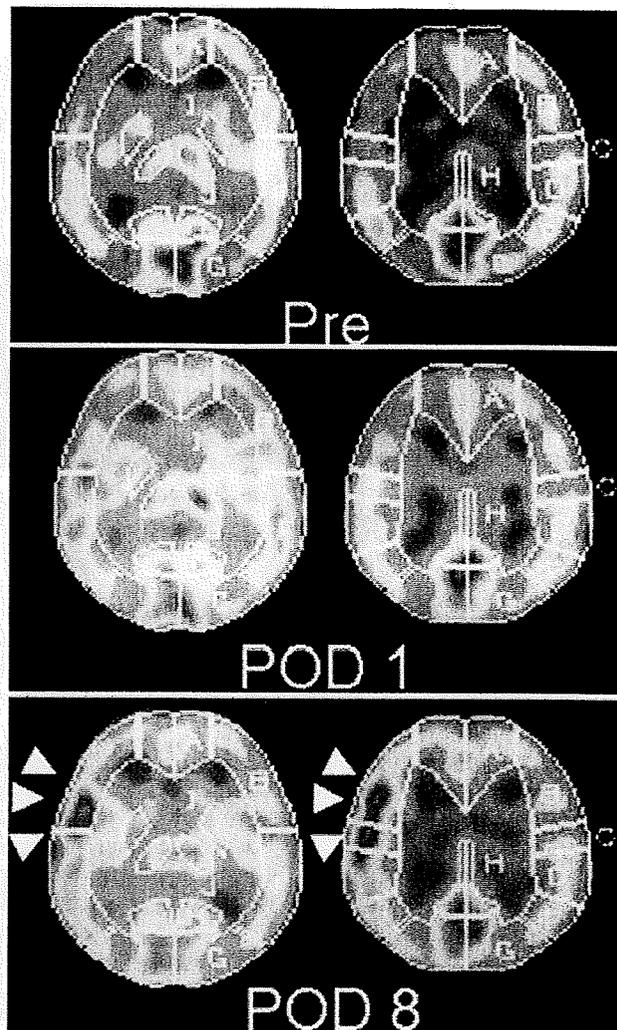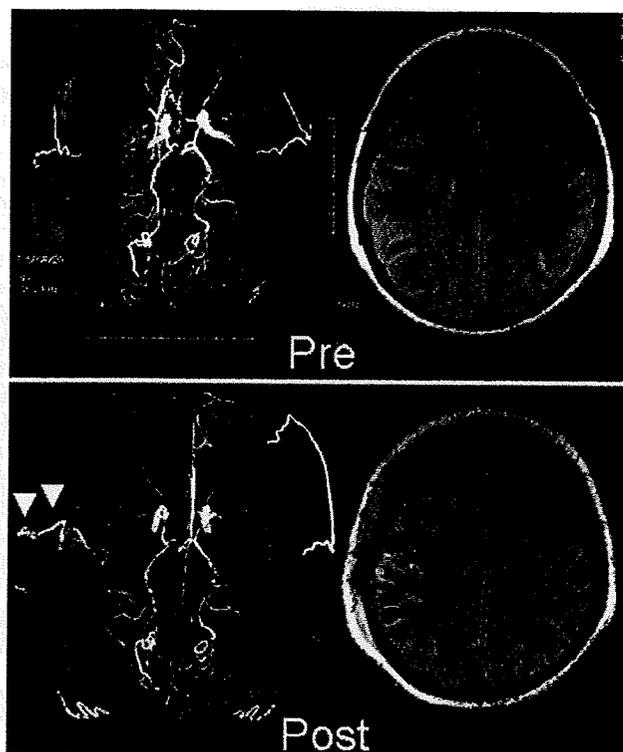
Fig. 7. *Upper Left:* Preoperative MR angiogram. *Upper Right:* Preoperative FLAIR study. *Lower Left:* Postoperative MR angiogram showing the apparently patent STA-MCA bypass *(arrowheads).* *Lower Right:* Postoperative FLAIR study showing high intensity signal around the site of anastomosis.
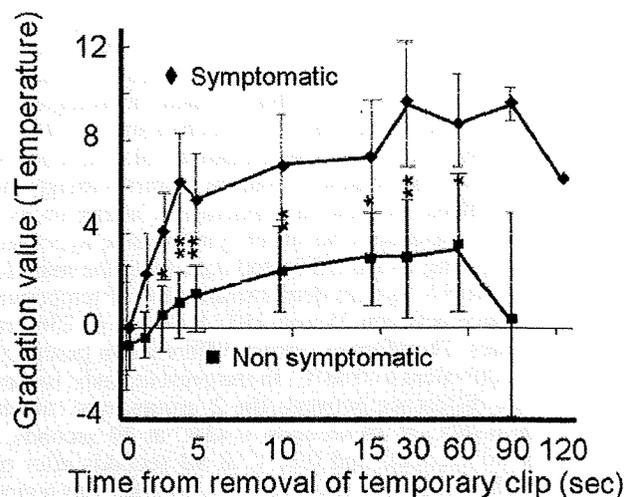

Fig. 8. Graph showing the differences in average gradation value within the ROI around the anastomosis site among 10 patients who had transient neurological deficits due to focal increase of CBF around the anastomosis site and 16 patients who did not, showing significant increase in gradation value (indirectly showing significant increase in surface cortical temperature) in the former group (up to 60 seconds after removal of the temporary clip). * p < 0.05; ** p < 0.05.

age gradation value change (representing temperature) was significantly higher in the patients who experienced symptomatic hyperperfusion (Fig. 8) immediately after and up to 60 seconds following removal of the temporary clip.

Discussion

In the present study, our novel infrared imaging system allowed us not only successful monitoring of the bypass patency and comprehensive visual evaluation of local hemodynamics, but also for the first time, it showed the possibility of estimating the risk of subsequent occurrence of postoperative symptomatic hyperperfusion by temperature rise around the anastomosis site during the operation.

Importance of Estimating Risk of Postoperative Symptomatic Hyperperfusion in Patients With Moyamoya Disease

Occurrence of transient postoperative neurological deficits due to hyperperfusion has been recently recognized as an important potential complication after revascularization surgery for moyamoya disease.[5–8,16] It is important to recognize the pathology because strict control of blood pressure is mandatory in patients with hyperperfusion, whereas such treatment is contradictory to that in patients with ischemic episodes.[5–7] In addition, from

the viewpoint of cognitive functional impairment, the occurrence of hyperperfusion cannot be ignored.[16] The rate of hyperperfusion in the present series was higher than that reported in the series dealing with STA-MCA anastomosis in chronic cerebral ischemia. Postoperative cerebral hyperperfusion syndrome has been considered to be less common in patients with moyamoya disease because of the relatively low-flow revascularization obtained through surgery for moyamoya disease. In our previous study involving 34 consecutive cases of moyamoya disease, we reported that STA-MCA anastomosis in patients with adult-onset moyamoya disease can result in a substantial rate (13 [38.2%] of 34) of temporary neurological deterioration due to transient focal intense increases in CBF at the site of anastomosis and that intensive blood pressure control can relieve this condition.[5] However, the clinical manifestation is different from hyperperfusion syndrome after carotid endarterectomy; radical clinical presentation succeeding intracranial hemorrhage was observed in 1 case, but the majority were limited to subtle, transient focal neurological deficits mimicking ischemic attack, with no patient suffering a permanent neurological deficit. Identification of the predictors for cerebral hyperperfusion in patients with moyamoya disease is clinically important. Preoperative cerebrovascular reserve capacity, severity of ischemia during surgery, patients age, and anatomical vascular structures around the site of the anastomosis may affect postoperative cerebral hyperperfusion.[5–8,10,16,19,25] In our study, most patients showed a preoperative cerebrovascular reserve capacity of < 0% (steal phenomenon), which may contribute to the high incidence of postoperative symptomatic hyperperfusion.

Regarding intraoperative ischemic insult during anastomosis, which may facilitate postischemic hyperperfusion, most of the cases were subjected to temporary

occlusion (30 minutes) at the distal M_4 segment. It is not clear how a rapid increase in CBF affects the ischemic brain in moyamoya disease, although a substantial number of patients may suffer transient neurological deterioration due to an unknown mechanism. As shown in the present study, the mean gradation value around the anastomosis site obtained from an infrared image showed a significant increase in temperature lasting up to 60 seconds in patients who suffer symptomatic hyperperfusion. According to the calibrated data from the manufacturer, the IRIS-V system demonstrates 20° of temperature difference between 25 and 45°C by 8-bit, or 256 gradation values. Therefore, a 1-point difference in gradation value is equivalent to 0.08°C. In the present study, the temperature difference between the 2 groups was calculated to be 0.28°C at 10 seconds, 0.42°C at 30 seconds, 0.41°C at 60 seconds, and 0.77°C at 90 seconds after removal of the temporary clip. However, whether this temperature increase is benign or a sign of abnormal overflow of CBF into a previously poorly perfused area, or merely a reaction unrelated to the postoperative phenomenon, is still uncertain. Even if it is a sign of abnormal overflow, the threshold remains unknown. Both issues are limitations of the present study and should be evaluated prospectively, and for a longer time after removal of the temporary clip. In light of the fact that STA-MCA anastomosis could result in postoperative symptomatic hyperperfusion in childhood[7] as well as in adult-onset moyamoya disease,[6] it is worth further studying the relationship between the pattern of intraoperative cerebral hemodynamics and postoperative neurological status.

Clinical Implications of Intraoperative Infrared Imaging

Infrared imaging is an established technique for studying the surface temperature of human organs.[18,23] In the past, this technique has been applied in coronary artery bypass graft surgery to measure the cooling effect of cardioplegic solutions, or to evaluate coronary perfusion and graft patency.[1,3,4] With advances in infrared technology, including detective wavelength, detective temperature range, cooling system, and filters, as well as data processing, it is now possible to observe surface blood flow with high spatial and time resolution without contact with blood vessels, radiation exposure, or injection of contrast medium.[21]

The relationship of infrared camera thermography and quantitative blood flow has been extensively investigated in the heart. Experimental cardiac studies demonstrated a quantitative correlation between blood flow and myocardial temperature.[1,3] In the isolated pig heart, in which there is no metabolic contribution to temperature change, graft flow was found to correlate highly with a mathematical expression of the temperature change observed during thermography.[3] In the brain literature, Watson et al.[24] applied high-resolution infrared imaging to the brain of *Cynomolgus* monkeys and reported that the cortical arterial temperature was related to blood flow and the temporal temperature profile was identical to that of blood flow measured by Doppler ultrasonography. Moreover, a recent study by Okada et al.[17] showed linear relationships between cortical surface CBF and

temperature that were confirmed using a laser Doppler flowmeter. It is considered that cortical brain temperature is determined by metabolism and blood flow coupling[2,9] and sensitive infrared imaging might be a useful measure provided that there is no significant metabolism change during monitoring.[24] Therefore, the increase in temperature around the anastomosis site in the present study was considered to be due to an increase in blood flow.

The IRIS-V is a new-generation infrared system with higher resolution at minimal temperature differences. In addition, by shifting the sensitive wavelength band up to 7–14 μm from 3–5 μm, it is possible to detect infrared rays from near the surface region. Using a previous prototype, we have evaluated patency of bypass in beagles (vessel diameter as small as 0.5 mm), and we have also reported that flow territory can be delineated by temperature difference.[14] Infrared monitoring has also been useful for confirmation of venous drainage during surgical obliteration of a spinal perimedullary arteriovenous malformation.[15] Including the novel infrared system presented in this report, future infrared monitoring will not only serve for intraoperative monitoring but may become a useful tool for estimation of postoperative risks, although further examination is necessary.

Conclusions

Temperature rise around an anastomosis site above a certain threshold during surgery as detected by intraoperative infrared monitoring might indicate the subsequent occurrence of postoperative symptomatic hyperperfusion. Prospective evaluation with a larger number of patients is necessary to validate this technique.

References

1. Adachi H, Becker LC, Ambrosio G, Takeda K, Dipaula AF, Baumgartner WA, et al: Assessment of myocardial blood flow by real-time infrared imaging. **J Surg Res 43:**94–102, 1987
2. Ecker RD, Goerss SJ, Meyer FB, Cohen-Gadol AA, Britton JW, Levine JA: Vision of the future: initial experience with intraoperative real-time high-resolution dynamic infrared imaging. Technical note. **J Neurosurg 97:**1460–1471, 2002

3. Falk V, Walther T, Kitzinger H, Rauch T, Diegeler A, Autschbach R, et al: An experimental approach to quantitative thermal coronary angiography. Thorac Cardiovasc Surg 46:25–27, 1998

4. Falk V, Walther T, Philippi A, Autschbach R, Krieger H, Dalichau H, et al: Thermal coronary angiography for intraoperative patency control of arterial and saphenous vein coronary artery bypass grafts: results in 370 patients. J Card Surg 10:147–160, 1995

5. Fujimura M, Kaneta T, Mugikura S, Shimizu H, Tominaga T: Temporary neurologic deterioration due to cerebral hyperperfusion after superficial temporal artery-middle cerebral artery anastomosis in patients with adult-onset moyamoya disease. Surg Neurol 67:273–282, 2007

6. Fujimura M, Kaneta T, Shimizu H, Tominaga T: Symptomatic hyperperfusion after superficial temporal artery-middle cerebral artery anastomosis in a child with moyamoya disease. Childs Nerv Syst 23:1195–1198, 2007

7. Fujimura M, Mugikura S, Shimizu H, Tominaga T: [Diagnostic value of perfusion-weighted MRI for evaluating postoperative alteration of cerebral hemodynamics following STA-MCA anastomosis in patients with moyamoya disease.] No Shinkei Geka 34:801–809, 2006 (Jpn)

8. Furuya K, Kawahara N, Morita A, Momose T, Aoki S, Kirino T: Focal hyperperfusion after superficial temporal artery-middle cerebral artery anastomosis in a patient with moyamoya disease. Case report. J Neurosurg 100:128–132, 2004

9. Gorbach AM, Heiss J, Kufta C, Sato S, Fedio P, Kammerer WA, et al: Intraoperative infrared functional imaging of human brain. Ann Neurol 54:297–309, 2003

10. Houkin K, Ishikawa T, Yoshimoto T, Abe H: Direct and indirect revascularization for moyamoya disease: surgical techniques and peri-operative complications. Clin Neurol Neurosurg 99 (Suppl 2):S142–S145, 1997

11. Ishikawa T, Houkin K, Kamiyama H, Abe H: Effects of surgical revascularization on outcome of patients with pediatric moyamoya disease. Stroke 28:1170–1173, 1997

12. Karasawa J, Kikuchi H, Furuse S, Kawamura J, Sakaki T: Treatment of moyamoya disease with STA-MCA anastomosis. J Neurosurg 49:679–688, 1978

13. Nakagawa A, Fujimura M, Ohki T, Suzuki H, Takayama K, Tominaga T: [Intraoperative brain surface blood flow monitoring using IRIS V thermographic imaging system in patients with Moyamoya disease.] No Shinkei Geka 34:1017–1025, 2006 (Jpn)

14. Nakagawa A, Hirano T, Uenohara H, Sato M, Kusaka Y, Shirane R, et al: Intraoperative thermal artery imaging of an EC-IC bypass in beagles with infrared camera with detectable wave-length band of 7-14 micron: possibilities as novel blood flow monitoring system. Minim Invasive Neurosurg 46:231–234, 2003

15. Nakagawa A, Hirano T, Uenohara H, Utsunomiya H, Suzuki S, Takayama K, et al: Use of intraoperative dynamic infrared imaging with detection wavelength of 7-14 micron in the surgical obliteration of spinal arteriovenous fistula: case report and technical considerations. Minim Invasive Neurosurg 47:136–139, 2004

16. Ogasawara K, Komoribayashi N, Kobayashi M, Fukuda T, Inoue T, Yamadate K, et al: Neural damage caused by cerebral hyperperfusion after arterial bypass surgery in a patient with moyamoya disease: case report. Neurosurgery 56:E1380, 2005

17. Okada Y, Kawamata T, Kawashima A, Hori T: Intraoperative application of thermography in extracranial-intracranial bypass surgery. Neurosurgery 60:362–366, 2007

18. Petibois C, Drogat B, Bikfalvi A, Deleris G, Moenner M: Chemical mapping of tumor progression by FT-IR imaging: towards molecular histopathology. Trends Biotechnol 24:455–462, 2006

19. Sakamoto T, Kawaguchi M, Kurehara K, Kitaguchi K, Furuya H, Karasawa J: Risk factors for neurologic deterioration after revascularization surgery in patients with moyamoya disease. Anesth Analg 85:1060–1065, 1997

20. Shirane R, Yoshida Y, Takahashi T, Yoshimoto T: Assessment of encephalo-galeo-myo-synangiosis with dural pedicle insertion in childhood moyamoya disease: characteristics of cerebral blood flow and oxygen metabolism. Clin Neurol Neurosurg 99 (Suppl 2):S79–S85, 1997

21. Suma H, Isomura T, Horii T, Sato T: Intraoperative coronary artery imaging with infrared camera in off-pump CABG. Ann Thorac Surg 70:1741–1742, 2000

22. Suzuki J, Takaku A: Cerebrovascular "moyamoya" disease. Disease showing abnormal net-like vessels in base of brain. Arch Neurol 20:288–299, 1969

23. Ueda M, Sakurai T, Kasai K, Ushikubo Y, Samejima H: Localisation of sensory motor cortex during surgery by changes of cortical surface temperature after median nerve stimulation. Lancet 350:561, 1997

24. Watson JC, Gorbach AM, Pluta RM, Rak R, Heiss JD, Oldfield EH: Real-time detection of vascular occlusion and reperfusion of the brain during surgery by using infrared imaging. J Neurosurg 96:918–923, 2002

25. Yoshimoto T, Houkin K, Kuroda S, Abe H, Kashiwaba T: Low cerebral blood flow and perfusion reserve induce hyperperfusion after surgical revascularization: case reports and analysis of cerebral hemodynamics. Surg Neurol 48:132–138, 1997

Address correspondence to: Atsuhiro Nakagawa, M.D., Department of Neurosurgery, Tohoku University Graduate School of Medicine, 1-1 Seiryo-machi, Aoba-ku, Sendai, Miyagi 980-8574, Japan. email: nakg_neurosurg@yahoo.co.jp.

ORIGINAL RESEARCH

N. Mori
S. Mugikura
S. Higano
T. Kaneta
M. Fujimura
A. Umetsu
T. Murata
S. Takahashi

The Leptomeningeal "Ivy Sign" on Fluid-Attenuated Inversion Recovery MR Imaging in Moyamoya Disease: A Sign of Decreased Cerebral Vascular Reserve?

BACKGROUND AND PURPOSE: Moyamoya disease is an idiopathic occlusive cerebrovascular disorder with abnormal microvascular proliferation. We investigated the clinical utility of leptomeningeal high signal intensity (ivy sign) sometimes seen on fluid-attenuated inversion recovery images in Moyamoya disease.

MATERIALS AND METHODS: We examined the relationship between the degree of the ivy sign and the severity of the ischemic symptoms in 96 hemispheres of 48 patients with Moyamoya disease. We classified each cerebral hemisphere into 4 regions from anterior to posterior. In 192 regions of 24 patients, we examined the relationship between the degree of the ivy sign and findings of single-photon emission CT, including the resting cerebral blood flow (CBF) and cerebral vascular reserve (CVR).

RESULTS: The degree of the ivy sign showed a significant positive relationship with the severity of the ischemic symptoms ($P < .001$). Of the 4 regions, the ivy sign was most frequently and prominently seen in the anterior part of the middle cerebral artery region. The degree of the ivy sign showed a negative relationship with the resting CBF ($P < .0034$) and a more prominent negative relationship with the CVR ($P < .001$).

CONCLUSIONS: The leptomeningeal ivy sign indicates decreased CVR in Moyamoya disease.

Moyamoya disease is an idiopathic cerebrovascular disorder characterized by bilateral steno-occlusive changes at or around the terminal part of the internal carotid arteries with abnormal vessel proliferation called "moyamoya" at the base of the brain.[1]

Leptomeningeal high signal intensity has sometimes been reported on unenhanced fluid-attenuated inversion recovery (FLAIR) MR imaging along the cerebral sulci or on the brain surface in this disease, which has been called the "ivy sign."[2]

A recent study found that the ivy sign was more prominent in the hemispheres with poorer visualization of the cortical branches of the middle cerebral artery (MCA) on MR angiography.[3] In addition, in our experience, a greater prominence of the ivy sign indicates more severe ischemic symptoms, which were found to decrease on follow-up MR images after effective revascularization surgery.

These findings prompted us to speculate that the degree of the ivy sign might be correlated with the severity of the ischemia. Therefore, to analyze the significance of the ivy sign as an indicator of ischemia, we recruited patients with focal ischemic symptoms. We then retrospectively examined the relationship between the degree of the ivy sign and the severity of the ischemic symptoms and compared it with the findings of single-photon emission CT (SPECT).

Materials and Methods

Patients

Between September 2003 and June 2007, 61 consecutive patients were diagnosed with Moyamoya disease according to the criteria of the Research Committee on Spontaneous Occlusion of the Circle of Willis (Moyamoya Disease) of the Ministry of Health and Welfare, Japan.[4] Of these patients, 11 with intracranial hemorrhage on CT at the onset of clinical symptoms and 2 with headache or dizziness alone were excluded. The remaining 48 patients with focal ischemic symptoms attributable to 1 cerebral hemisphere (14 males and 34 females ranging from 2 to 64 years of age, mean age 33 years) were included in this retrospective review.

Imaging Examinations

MR imaging was performed in these patients by using a 1.5T ($n = 32$; Signa Horizon LX CVi; GE Healthcare, Milwaukee, Wis) or 1T ($n = 16$; Signa Horizon LX; GE Healthcare) scanner. The MR imaging protocol included axial T1- and T2-weighted imaging, axial diffusion-weighted imaging, axial unenhanced FLAIR imaging, and 3D time-of-flight MR angiography. The FLAIR imaging was performed by using a fast inversion recovery sequence with TR, 9002 and 9002 ms; TE_{eff}, 120 and 117 ms; TI, 2200 and 2100 ms; section thicknesses, 5.9 and 6.9 mm; section gap, 1.0 and 1.0 mm; matrix, 320 × 224 and 320 × 192 on the 1.5 and 1T scanners, respectively.

Of 48 patients studied with iodine 123 N-isopropyl-p-iodoamphetamine (^{123}I-IMP)-SPECT, 18 had qualitative SPECT only, whereas the other 30 underwent quantitative SPECT by using a table look-up method (resting SPECT).[5,6] A SPECT scanner (SPECT 2000H; Hitachi Medical, Tokyo, Japan) with a 4-head rotating gamma camera was used for all SPECT studies. In 24 of the aforementioned 30 patients, ^{123}I-IMP-SPECT with an acetazolamide injection (ACZ-SPECT) followed at an interval of 2–7 days. This means that
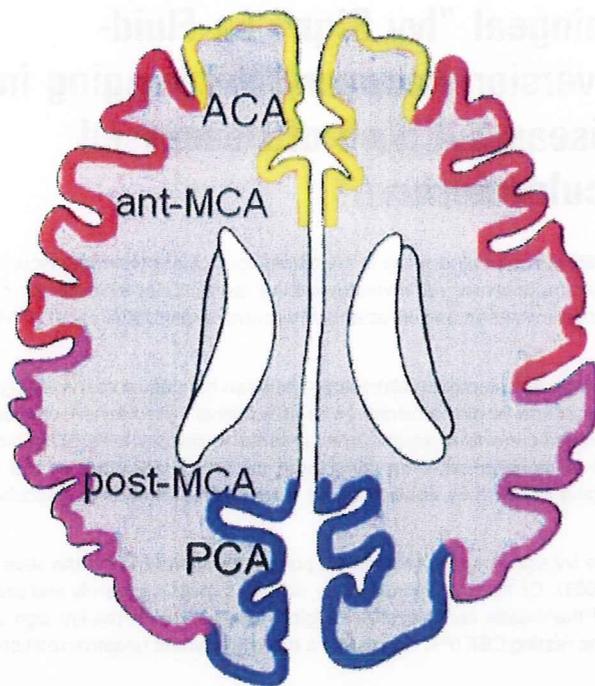
Fig 1. Classification of 4 corticosubcortical regions in each cerebral hemisphere at the level of the body of the lateral ventricle: the region of the ACA, the ant-MCA, the post-MCA, and the PCA.

ACZ-SPECT was not performed in the remaining 6 patients at all because the ACZ injection might have worsened the ischemic symptoms in 3 patients who experienced a completed stroke (CS) within 1 month. Two patients had frequent transient ischemic attacks (TIAs), and machine failure precluded performing the examination in the remaining patient.

The ^{123}I-IMP (111 MBq, 3 mCi) was injected intravenously from the antecubital vein. After 10 minutes, 1 arterial blood sample was taken to calibrate the previously determined standard input function, and the radioactivity concentration in whole blood was counted by using a well counter that was cross-calibrated to the SPECT scanner. A single SPECT scan was obtained at a midscan time of 30 minutes after ^{123}I-IMP administration. In the 2-compartment analysis of ^{123}I-IMP, the distribution volume, which is the ratio of the influx constant to the efflux constant, could be set between 40 and 45 mL. The cerebral blood flow (CBF) was calculated pixel by pixel (128 × 128 matrix) on the basis of single-SPECT data and a standard input function was calibrated by using a 1-point arterial blood sample. By administering ACZ (1000 mg/individual intravenously) 10 minutes before the ^{123}I-IMP infusion, ACZ-activated CBF (ACZ-CBF) maps were also obtained.

Imaging Analysis

Ivy Sign Scores on FLAIR Images. The ivy sign on FLAIR images was defined as a linear high signal intensity along the cortical sulci or brain surface in the cerebral hemisphere. The corticosubcortical region of each cerebral hemisphere was divided into the following 4 regions adapted from a previous report (Fig 1)[7]: the region of the anterior cerebral artery (ACA), the anterior half of the MCA region (ant-MCA), the posterior half of the MCA region (post-MCA), and the region of the posterior cerebral artery (PCA). The ant-MCA and post-MCA regions were separated by the central sulcus, with the tem-

poral lobe belonging to the post-MCA. The degree of the ivy sign (ivy sign score) in each region was classified into 3 grades (0–2), where grade zero indicated an absence of the ivy sign, grade 1 indicated that the ivy sign was seen on less than half of the cortical surface in each region, and grade 2 indicated that the ivy sign was seen on more than half of the cortical surface. The ivy sign was scored subjectively by reviewing all the FLAIR images traversing all the cerebral hemispheres.

The scoring immediately along the infarcted cortices was considered uninterpretable. Therefore, in 9 regions harboring foci of cortical infarcts, the sign over the remaining uninvolved part was estimated and recorded as the score for those regions. Conversely, in 6 regions with white matter infarcts, the ivy sign over the cortex was graded irrespective of the infarct as long as its overlying cortex was spared. The scores for each region were summed in each hemisphere and are defined as the ivy sign score for that individual hemisphere.

Two neuroradiologists (with 7 and 15 years of experience) reviewed the ivy sign independently without knowledge of the clinical information or SPECT findings. Initial interobserver agreement was 87% in interpreting FLAIR images. When the initial interpretation differed between the 2 raters, the final interpretation was reached by consensus. A case illustrating the grading of the ivy sign is shown in Fig 2.

Types of Hemisphere According to Ischemic Symptoms. We classified the 96 cerebral hemispheres of the 48 patients into 4 grades of focal ischemic symptoms according to the Research Committee on Spontaneous Occlusion of the Circle of Willis (Moyamoya Disease) of the Ministry of Health and Welfare, Japan[4]: asymptomatic (AS), TIA, frequent TIAs, and CS. Accordingly, the respective hemispheres were called AS, TIA, frequent TIAs, and CS.

Focal ischemic symptoms lasting <24 hours were defined as a TIA, whereas TIAs more than twice a month were defined as frequent TIAs and focal symptoms for >24 hours were CS.

Quantification of Regional CBF and Cerebral Vascular Reserve. We quantified the CBF without activation (resting CBF) and ACZ-CBF. Next, the cerebral vascular reserve (CVR), which is defined as the percentage difference between the ACZ-CBF and the resting CBF compared with the resting CBF, was calculated as follows[8-10]:

$$CVR(\%) = [(ACZ\text{-}CBF - resting\ CBF)/resting\ CBF] \times 100.$$

The resting CBF and ACZ-CBF were converted by using fully automated region-of-interest–based analysis software called a 3D stereotactic region of interest template (3D-SRT). 3D-SRT is software that was designed to perform region-of-interest analysis of the brain by using anatomic standardization. This method allows region-of-interest analysis of the brain with improved objectivity and excellent reproducibility.[11,12] The 3D-SRT software obtains the regional CBF in the corticosubcortical regions of each cerebral hemisphere (SRT-CBF) for the 8 regions of interest for which the respective volumes are known (regions of interest A–H, Fig 3).

To match our study design, we recalculated both the resting CBF and ACZ-CBF for the 4 regions (ACA, ant-MCA, post-MCA, and PCA). In our study, these were represented by region of interest A, region of interest B + region of interest C, region of interest D + region of interest E + region of interest F, and region of interest G + region of interest H, respectively. In this recalculation, region of interest H, which might partially include the ACA region, was regarded as within the PCA region.

At this recalculation, the correction was made proportional to the
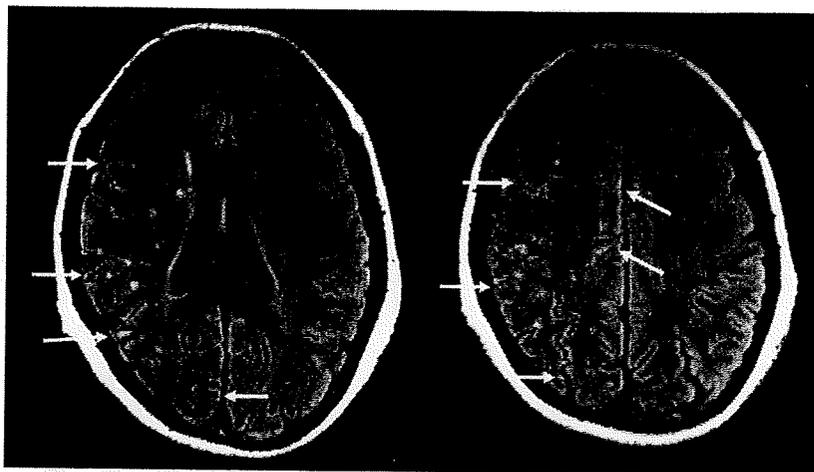
Fig 2. A 47-year-old woman with frequent transient left upper and lower motor weakness. Arrows indicate the ivy sign. The ivy sign score of the right side is 1 in the ACA and PCA regions, respectively, and 2 in the ant-MCA and post-MCA regions, respectively. No ivy sign is seen on the left side. The ivy sign score in individual hemispheres is 6 on the right side and zero on the left side.
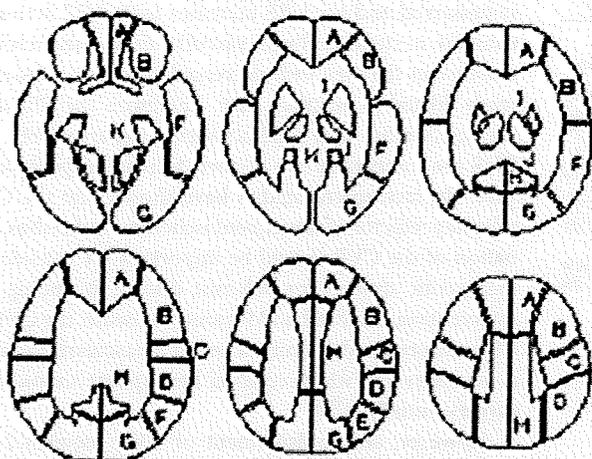
Fig 3. The template of constant regions of interest for the 3D-SRT. A representative 6 sections of the template are shown: A, callosomarginal; B, precentral; C, central; D, parietal; E, angular; F, temporal; G, posterior cerebral; H, pericallosal; I, basal ganglia; J, thalamus; K, hippocampus; L, cerebellum. Adapted from Takeuchi R et al.[11]

Fig 4. Bar graph shows the ivy sign score of each type of hemispheric symptom. The ivy sign scores show significant positive correlation with the grades of clinical types of hemispheric symptoms ($P < .001$).

volume of each region of interest within a certain region, as follows:

$$\text{CBF in Ant-MCA} = [VB/(VB + VC)] \times$$
$$[\text{CBF in region of interest B}] +$$
$$[VC/(VB + VC)] \times [\text{CBF in region of interest C}],$$

where VB is the volume of region of interest B and VC is the volume of region of interest C.

Four regions of interest (in 3 patients), which contained cortical infarctions on MR imaging, were excluded from this summation, though the regions of interest with white matter infarcts alone were not excluded.

Statistical Analysis

We examined the relationship between the ivy sign score of individual hemispheres and the types of hemispheric symptom. Finally, we examined the relationship between the ivy sign score with the resting CBF and CVR on SPECT in a total of 192 regions of 24 patients. For statistical analysis, the Spearman rank correlation coefficient was determined by using the software package JMP 4J (SAS Institute, Tokyo, Japan), with $P < .05$ considered statistically significant.

Results

The ivy sign scores showed a significant positive correlation with the grade of the clinical type of hemispheric symptom (eg, AS, TIA, frequent TIA, CS) (Fig 4, $P < .001$). The score increased as the clinical symptoms became more severe (ie, from AS to CS). The ivy sign score according to the 4 cortico-subcortical regions is shown in Fig 5. Both the frequency of positive ivy signs and its score were highest in the ant-MCA region, from which they decreased significantly going posteriorly toward the PCA region ($P < .001$).

Regarding the relationship between the ivy sign scores and the SPECT findings, the resting CBF decreased significantly, though slightly, as the ivy sign score increased (Table, $P = .0034$) (Fig 6). A more obvious negative correlation was found

Fig 5. Bar graph shows the ivy sign score according to 4 cortico-subcortical regions, each color indicating a different grade. Each color represent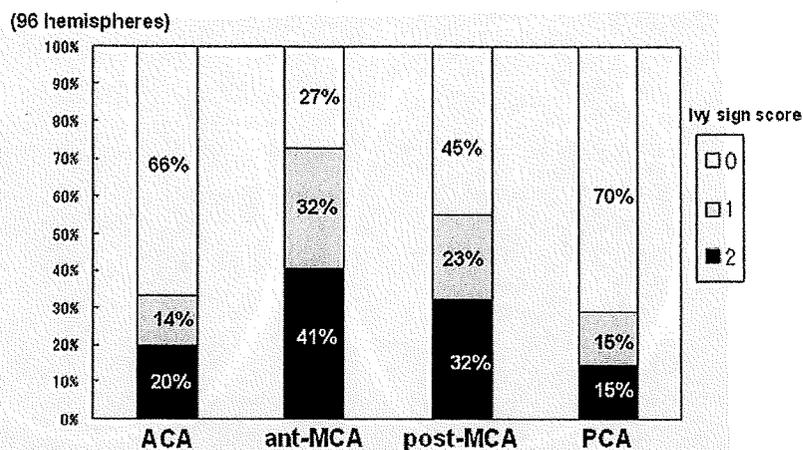s the percentage of the score in the hemisphere compared with all 96 hemispheres for each ivy sign score. The number along the each color represents the score.

The relationship between the ivy sign score and SPECT findings*		
Ivy Sign Score (No. of Regions)	Resting CBF (mL/100 g/min), Median (25th Percentile, 75th Percentile)	CVR (%), Median (25th Percentile, 75th Percentile)
0 (115)	33.3 (30.4, 37.2)	9.1 (1.8, 30.1)
1 (37)	32.4 (28.6, 35.0)	4.3 (−5.7, 21.5)
2 (40)	31.6 (28.2, 33.6)	−0.2 (−7.4, 5.3)

Note:—SPECT indicates single-photon emission CT; CBF, cerebral blood flow; CVR, cerebral vascular reserve.
* As the ivy sign score increased, the median value of the resting CBF decreased slightly ($P = .0034$). On the other hand, as the ivy sign score increased, the median value of the CVR decreased more obviously ($P < .001$).

between the score and the CVR (Table, $P < .001$) (Fig 6): a higher ivy sign score signified a correspondingly lower CVR.

Discussion

Diffuse leptomeningeal enhancement in contrast-enhanced T1-weighted images in patients with Moyamoya disease was first reported by Ohta et al.[13] The pattern of contrast enhancement resembled ivy creeping on stones and was named the ivy sign. Subsequently, similar leptomeningeal high signal intensity was reported on unenhanced FLAIR images and was also referred to as the ivy sign.[2,14]

In this study, we evaluated the ivy sign on FLAIR images in patients with focal ischemic symptoms and found a significant positive correlation between the severity of these symptoms and the degree of the ivy sign. Furthermore, the ivy sign was found to indicate decreased CVR in Moyamoya disease noninvasively. This decrease in CVR may be related to the presenting ischemic symptoms, the severity of which was found to be correlated with the degree of the ivy sign. Regarding the distribution of the ivy sign, the high prevalence in the ant-MCA region was consistent with previous SPECT studies reporting that the CVR in the ant-MCA region tended to be most severely decreased.[8-10] In contrast, the CVR was relatively preserved in the ACA region and posterior part of the cerebral hemisphere. This might be explained by the frequent development of transdural collaterals from the ophthalmic artery[7,15,16] and leptomeningeal collaterals from the less involved PCA.[7,17,18]

In general, the CVR is measured by using ACZ, a cerebral

vasculature dilator. In normal areas, its vasodilatory capacity is preserved and the CBF increases with ACZ activation. In contrast, in steno-occlusive vascular disease, the cerebral vasculature in the area with decreased perfusion pressure is already dilated to maintain CBF. Therefore, the CBF does not increase further with ACZ activation (ie, areas with reduced CVR are susceptible to a further decrease in perfusion pressure). In fact, recent studies have shown that the CVR is a reliable predictor of subsequent ischemic stroke; thus, an evaluation of the CVR should be important for considering the therapeutic strategy for ischemic disease, including surgical intervention.[19] Indeed, in Moyamoya disease, the CVR is usually measured to determine whether revascularization surgery is necessary and which cerebral hemisphere should undergo surgery initially.[8,20,21]

However, any measurement of CVR requires 2 SPECT evaluations, including resting and ACZ activation studies, which may be burdensome to patients, and ACZ activation may cause side effects such as headache and a feeling of discomfort.[19,22] Especially in patients with a very severe decrease in CVR, the administration of ACZ sometimes causes a further reduction in CBF due to the vascular steal phenomenon to the adjacent area with relatively preserved CVR.[19,22] Therefore, ACZ should be administered cautiously in patients with severe ischemic symptoms. Indeed, in 5 of the 30 patients in our study, ACZ activation was not performed for fear of worsening their ischemic symptoms via the steal phenomenon. In such cases, observation of the ivy sign on FLAIR images may help to assess the CVR noninvasively in Moyamoya disease. Of course, we do not mean to imply that quantitative SPECT is totally replaceable by evaluating the ivy sign, which is subjective. However, it would be beneficial if the CVR could be predicted from routine MR imaging sequences.

As for the mechanism leading to the development of the ivy sign, previous reports speculated that this sign was likely to reflect slow retrograde flow of engorged pial collateral arteries via leptomeningeal anastomosis,[2] an opinion with which we do not completely agree. In general, the leptomeningeal collaterals are developed among the distal cortical branches of the ACA, MCA, and PCA. In Moyamoya disease, however, lepto-
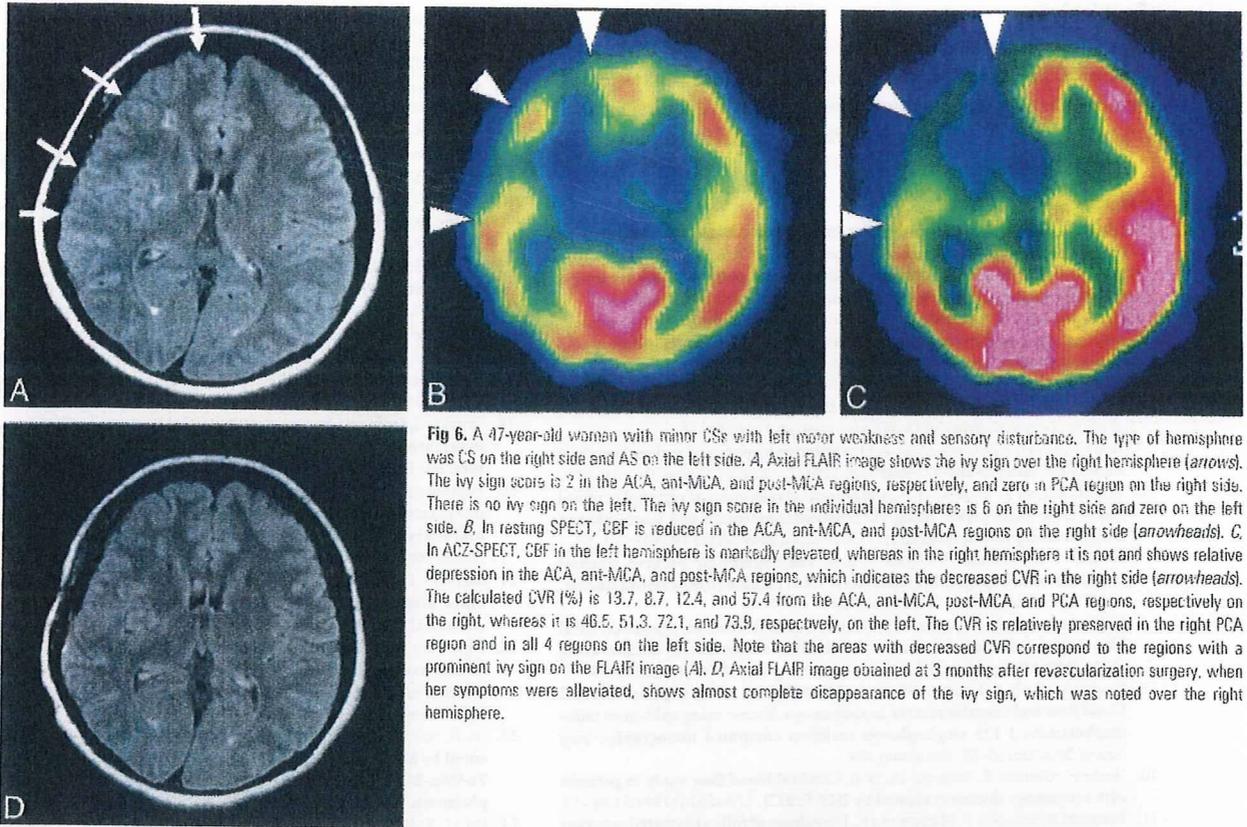
Fig 6. A 47-year-old woman with minor CSs with left motor weakness and sensory disturbance. The type of hemisphere was CS on the right side and AS on the left side. *A,* Axial FLAIR image shows the ivy sign over the right hemisphere (*arrows*). The ivy sign score is 2 in the ACA, ant-MCA, and post-MCA regions, respectively, and zero in PCA region on the right side. There is no ivy sign on the left. The ivy sign score in the individual hemispheres is 6 on the right side and zero on the left side. *B,* In resting SPECT, CBF is reduced in the ACA, ant-MCA, and post-MCA regions on the right side (*arrowheads*). *C,* In ACZ-SPECT, CBF in the left hemisphere is markedly elevated, whereas in the right hemisphere it is not and shows relative depression in the ACA, ant-MCA, and post-MCA regions, which indicates the decreased CVR in the right side (*arrowheads*). The calculated CVR (%) is 13.7, 8.7, 12.4, and 57.4 from the ACA, ant-MCA, post-MCA, and PCA regions, respectively on the right, whereas it is 46.5, 51.3, 72.1, and 73.9, respectively, on the left. The CVR is relatively preserved in the right PCA region and in all 4 regions on the left side. Note that the areas with decreased CVR correspond to the regions with a prominent ivy sign on the FLAIR image (*A*). *D,* Axial FLAIR image obtained at 3 months after revascularization surgery, when her symptoms were alleviated, shows almost complete disappearance of the ivy sign, which was noted over the right hemisphere.

meningeal collaterals are mainly developed from the PCA and extend forward to the territory of the anterior circulation, because the terminal part of internal carotid artery and proximal ACA/MCA are involved in the steno-occlusive process.[6] Accordingly, the leptomeningeal collaterals from the PCA are more developed in the posterior part of the cerebral hemisphere, which should be shown as a higher ivy sign in the post-MCA region if the ivy sign really reflected leptomeningeal collaterals from the PCA. However, the ivy sign score was higher in the ant-MCA region in this study; therefore, we doubt this hypothesis.

Our results showed that a positive ivy sign reflected a decreased CVR by SPECT. That is why we suspect that the ivy sign reflects maximally dilated pial vasculature to compensate for the decreased perfusion pressure rather than the leptomeningeal collateral arteries. In fact, when a craniotomy is performed in patients with Moyamoya disease, we observe the extremely dilated fine pial vasculature at the surface of the brain, which might be the source of the sign (Fig. 7). Another possible correlate of the ivy sign raised in the previous literature was the congested thickening of the leptomeninges, which is often seen on the brain surface in this disease (Fig. 7).[1,2] Although we admit that this can also be contributory, its exact relationship to the ivy sign remains to be clarified.

There are some limitations in our study. The FLAIR images were obtained by using 2 different scanners of different field strengths (1T and 1.5T). The appearance of the ivy sign may be different according to the field strength, which remains unclarified.

Next, we assessed the relationship between the ivy sign and SPECT findings in each region respectively, on the assumption

Fig 7. A 36-year-old man with Moyamoya disease. Extremely dilated fine pial vasculature and opaque thickened leptomeninges are seen on the brain surface when a craniotomy is performed.

that the 4 different regions had an equal reference value. Strictly speaking, however, both CBF and CVR should have different reference values according to different regions of the brain (ie, frontal and occipital lobes normally have different values of CBF and CVR).[23,24]

Finally, the 4 regions of each cerebral hemisphere for evaluating the ivy sign score did not completely correspond to the regions of interest for CBF and CVR recalculated. This incomplete correspondence might have been derived from having used the template. However, we believe that the assessment was made rather objectively by this automatic region-of-interest process using the templates.

Conclusions

Our findings showed that the ivy sign on FLAIR can reveal decreased CVR in Moyamoya disease. This sign may help to determine the need for surgery and is useful in predicting noninvasively the CVR before and after revascularization surgery.

References

1. Suzuki J, Takaku A. Cerebrovascular "moyamoya" disease: disease showing abnormal net-like vessels in base of brain. *Arch Neurol* 1969;20:288–99
2. Maeda M, Tsuchida C. "Ivy sign" on fluid-attenuated inversion-recovery images in childhood moyamoya disease. *AJNR Am J Neuroradiol* 1999;20:1836–38
3. Fujiwara H, Momoshima S, Kuribayashi S. Leptomeningeal high signal intensity (ivy sign) on fluid-attenuated inversion-recovery (FLAIR) MR images in moyamoya disease. *Eur J Radiol* 2005;55:224–30
4. Fukui M. *Annual Report 1993: The Research Committee on Spontaneous Occlusion of the Circle of Willis (Moyamoya Disease) of the Ministry of Health and Welfare.* Tokyo: Ministry of Health and Welfare; 1994:122–24
5. Iida H, Itoh H, Nakazawa M, et al. Quantitative mapping of regional cerebral blood flow using iodine-123-IMP and SPECT. *J Nucl Med* 1994;35:2019–30
6. Iida H, Akutsu T, Endo K, et al. A multicenter validation of regional cerebral blood flow quantitation using [123I]iodoamphetamine and single photon emission computed tomography. *J Cereb Blood Flow Metab* 1996;16:781–93
7. Mugikura S, Takahashi S, Higano S, et al. The relationship between cerebral infarction and angiographic characteristics in childhood moyamoya disease. *AJNR Am J Neuroradiol* 1999;20:336–43
8. Nakagawara J, Takeda R, Suematsu K, et al. Quantification of regional cerebral blood flow and vascular reserve in childhood moyamoya disease using [123I]IMP-ARG method. *Clin Neurol Neurosurg* 1997;99(suppl 2):S96–99
9. Honda M, Ezaki Y, Kitagawa N, et al. Quantification of the regional cerebral blood flow and vascular reserve in moyamoya disease using split-dose iodoamphetamine I 123 single-photon emission computed tomography. *Surg Neurol* 2006;66:155–59, discussion 159
10. Hoshi H, Ohnishi T, Jinnouchi S, et al. Cerebral blood flow study in patients with moyamoya disease evaluated by IMP SPECT. *J Nucl Med* 1994;35:44–50
11. Takeuchi R, Sengoku T, Matsumura K. Usefulness of fully automated constant ROI analysis software for the brain: 3DSRT and FineSRT. *Radiat Med* 2006;24:538–44
12. Takeuchi R. Fully automated ROI analysis software for the brain; 3DSRT [in Japanese]. *Nippon Hoshasen Gijutsu Gakkai Zasshi* 2003;59:1462–74
13. Ohta T, Tanaka H, Kuroiwa T. Diffuse leptomeningeal enhancement, "ivy sign," in magnetic resonance images of moyamoya disease in childhood: case report. *Neurosurgery* 1995;37:1009–12
14. Yoon HK, Shin HJ, Chang YW. "Ivy sign" in childhood moyamoya disease: depiction on FLAIR and contrast-enhanced T1-weighted MR images. *Radiology* 2002;223:384–89
15. Suzuki J, Kodama N. Cerebrovascular "moyamoya" disease. 2: collateral routes to forebrain via ethmoid sinus and superior nasal meatus. *Angiology* 1971;22:223–36
16. Satoh S, Shibuya H, Matsushima Y, et al. Analysis of the angiographic findings in cases of childhood moyamoya disease. *Neuroradiology* 1988;30:111–19
17. Yamada I, Murata Y, Umehara I, et al. SPECT and MRI evaluations of the posterior circulation in moyamoya disease. *J Nucl Med* 1996;37:1613–17
18. Mugikura S, Takahashi S, Higano S, et al. Predominant involvement of ipsilateral anterior and posterior circulations in moyamoya disease. *Stroke* 2002;33:1497–500
19. Settakis G, Molnar C, Kerenyi L, et al. Acetazolamide as a vasodilatory stimulus in cerebrovascular diseases and in conditions affecting the cerebral vasculature. *Eur J Neurol* 2003;10:609–20
20. Fujimura M, Kaneta T, Mugikura S, et al. Temporary neurologic deterioration due to cerebral hyperperfusion after superficial temporal artery-middle cerebral artery anastomosis in patients with adult-onset moyamoya disease. *Surg Neurol* 2007;67:273–82
21. McAuley DJ, Poskitt K, Steinbok P. Predicting stroke risk in pediatric moyamoya disease with xenon-enhanced computed tomography. *Neurosurgery* 2004;55:327–32, discussion 332–33
22. Kuwabara Y, Ichiya Y, Sasaki M, et al. Time dependency of the acetazolamide effect on cerebral hemodynamics in patients with chronic occlusive cerebral arteries: early steal phenomenon demonstrated by [^{15}O]H$_2$O positron emission tomography. *Stroke* 1995;26:1825–29
23. Ito H, Inoue K, Goto K. Database of normal human cerebral blood flow measured by SPECT. I. Comparison between I-123-IMP, Tc-99m-HMPAO, and Tc-99m-ECD as referred with O-15 labeled water PET and voxel-based morphometry. *Ann Nucl Med* 2006;20:131–08
24. Ito H, Yokoyama I, Iida H, et al. Regional differences in cerebral vascular response to P$_a$CO$_2$ changes in humans measured by positron emission tomography. *J Cereb Blood Flow* 2000;20:1264–70

A rare Asian founder polymorphism of *Raptor* may explain the high prevalence of Moyamoya disease among East Asians and its low prevalence among Caucasians

Wanyang Liu · Hirokuni Hashikata · Kayoko Inoue · Norio Matsuura · Yohei Mineharu ·
Hatasu Kobayashi · Ken-ichiro Kikuta · Yasushi Takagi · Toshiaki Hitomi · Boris Krischek ·
Li-Ping Zou · Fang Fang · Roman Herzig · Jeong-Eun Kim · Hyun-Seung Kang ·
Chang-Wan Oh · David-Alexandre Tregouet · Nobuo Hashimoto · Akio Koizumi

Abstract

Background In an earlier study, we identified a locus for Moyamoya disease (MMD) on 17q25.3.

Methods Linkage analysis and fine mapping were conducted for two new families in additional to the previously studied 15 families. Three genes, *CARD14*, *Raptor*, and *AATK*, were selected based on key words, namely, "inflammation", "apoptosis", "proliferation", and "vascular system", for further sequencing. A segregation analysis of 34 pedigrees was performed, followed by a case–control study in Japanese (90 cases vs. 384 controls), Korean (41 cases vs. 223 controls), Chinese (23 cases and 100 controls), and Caucasian (25 cases and 164 controls) populations.

Results Linkage analysis increased the LOD score from 8.07 to 9.67 on 17q25.3. Fine mapping narrowed the linkage signal to a 2.1-Mb region. Sequencing revealed that only one newly identified polymorphism, ss161110142, which was located at position −1480 from the transcription site of the *Raptor* gene, was common to all four unrelated sequenced familial affected individuals. ss161110142 was then shown to segregate in the 34 pedigrees studied, resulting in a two-point LOD score of 14.2 ($P =$ 3.89×10^{-8}). Its penetrance was estimated to be 74.0%. Among the Asian populations tested (Japanese, Korean, and Chinese), the rare allele was much more frequent in cases (26, 33, and 4%, respectively) than in controls (1, 1, and 0%, respectively) and was associated with an increased odds ratio of 52.2 (95% confidence interval 27.2–100.2) ($P = 2.5 \times 10^{-49}$). This allele was, however, not detected

W. Liu, H. Hashikata and K. Inoue have contributed equally to this study.

Electronic supplementary material The online version of this article (doi:10.1007/s12199-009-0116-7) contains supplementary material, which is available to authorized users.

W. Liu · H. Hashikata · K. Inoue · N. Matsuura ·
Y. Mineharu · H. Kobayashi · T. Hitomi · A. Koizumi (✉)
Department of Health and Environmental Sciences,
Kyoto University Graduate School of Medicine, Konoe-cho,
Yoshida, Sakyo-ku, Kyoto 606-8501, Japan
e-mail: koizumi@pbh.med.kyoto-u.ac.jp

H. Hashikata · Y. Mineharu · K. Kikuta · Y. Takagi ·
N. Hashimoto
Department of Neurosurgery,
Kyoto University Graduate School of Medicine, Kyoto, Japan

B. Krischek
Department of Neurosurgery,
University of Tübingen, Tübingen, Germany

L.-P. Zou
Department of Pediatrics, Chinese People's Liberation Army
General Hospital, Beijing, China

F. Fang
Beijing Children's Hospital, Capital Medical University,
Beijing, China

R. Herzig
Department of Neurology, Stroke Center, Faculty of Medicine
and Dentistry, Palacky University and University Hospital,
Olomouc, Czech Republic

J.-E. Kim · H.-S. Kang · C.-W. Oh
Department of Neurosurgery, Seoul National University College
of Medicine, Seoul, Korea

D.-A. Tregouet
Institut National de la Santé et de la Recherche Médicale
(INSERM), UMRS_937, Université Pierre et Marie Curie,
Paris 6, Paris, France

in the Caucasian samples. Its population attributable risk was estimated to be 49% in the Japanese population, 66% in the Korean population, and 9% in the Chinese population.

Conclusion ss161110142 may confer susceptibility to MMD among East Asian populations.

Keywords Association studies in genetics · Cerebral stroke · Childhood stroke · Genetic linkage · Moyamoya disease

Introduction

Moyamoya disease (MMD: MIM%607151) is an idiopathic disorder characterized by steno-occlusive lesions around the terminal portions of the internal carotid arteries accompanied by collateral vessels (moyamoya vessels) [1].

While the incidence of MMD is worldwide [2], it is particularly high in East Asian countries, such as Japan, Korea, and China [3, 4]. In Japan, the most recent prevalence and annual incidence statistics were reported to be 10.5 and 0.94 per 100,000 persons, respectively [3]. In comparison, the incidence in Europe is estimated to be about one-tenth of that in Japan [3, 4], while in the USA, the incidence is about 0.086 per 100,000 persons and is higher among Asian Americans and African Americans than among Caucasian Americans [3, 4]. MMD has been attracting increasing attention as an important cause of cerebral stroke in children [5].

There is epidemiological evidence that about 15% of MMD patients have familial occurrence [6, 7]. A recent genome-wide linkage analysis identified a susceptibility locus for MMD at 17q25.3 [8]. The primary aim of the study reported here was to carry out positional cloning for MMD at the 17q25.3 locus. Based on our results, we report here the identification of a rare variant within the promoter of the *Raptor* gene that appears to be a strong candidate for MMD among East Asians.

Methods

Study population

The study was approved by the Ethics Committee of the Kyoto University Institutional Review Board, and written informed consent was obtained from all subjects. Two groups of case participants were enrolled in this study. The first group comprised familial participants selected to join this study because of the presence of more than one case among blood relatives. Specifically, 194 family members with 36 Japanese probands and five family members with one Korean proband were enrolled in this study. Medical records pertaining to vascular diseases and risk factors were collected from all of the family members for verification of the diagnosis. The two new families joined this study after the first linkage study had been completed.

Members of the probands' families admitted to Kyoto University Hospital or any of the other hospitals collaborating in this study were recruited. With the patients' consent, samples and clinical data were collected, de-identified and banked.

The second group comprised singular participants who joined this study as single cases without affected blood relatives. Irrespective of the family histories, single patients who joined without affected blood relatives were classified as singular participants. These cases were recruited from Kyoto University (*n* = 90), Seoul National University in Korea (*n* = 41), the Chinese People's Liberation Army General Hospital and Capital Medical University in China (*n* = 23), Tubingen University in Germany (*n* = 21), and the Stroke Center, Department of Neurology, Palacky University and University Hospital Olomouc in the Czech Republic (*n* = 4). Panels of 384 Japanese, 223 Korean, 100 Chinese, and 164 Caucasian (mostly German) participants were selected from the same respective centers as for singular cases to serve as controls for this study. Magnetic resonance angiography (MRA) screening was carried out for all Japanese controls, but not for all of the Korean, Chinese, and Caucasian controls. The small incidence of MMD in the general population was assumed not to affect the results of the association study.

The diagnosis of MMD for the probands of the families or singular participants was rigorously based on the Japanese criteria, the so-called RCMJ (Research Committee on Moyamoya Disease of the Ministry of Health, Welfare and Labor, Japan) criteria (Table 1) [9]. A number of the familial participants other than the probands who did not satisfy the RCMJ criteria were nevertheless classified as MMD cases because they met the "broad" classification (Table 1) [8].

Linkage analysis and haplotype estimation

Two additional families (pedigrees 19 and 20) were genotyped (Fig. 1). It should be noted that family number 12 was vacant for the previously reported linked locus [8]. Genotyping, mapping, and haplotype estimation were conducted as previously reported [8]. Briefly, genomic DNA was extracted from blood samples from living patients using a QIAamp DNA Blood Mini kit (Qiagen, Hilden, Germany).

A total of 13 markers (D17S2195, D17S1847, D17S1806, D17S784, rs2071148, rs2280147, rs2293099, D17S704, D17S668, D17S928, rs2291395, rs2279395, and

Table 1 Diagnostic criteria of Moyamoya disease

RCMJ criteria: all of the following findings:

Steno-occlusive lesions around the terminal portions of the internal carotid arteries
(including the proximal portions of the anterior cerebral arteries and middle cerebral arteries)

Moyamoya vessels at the base of the brain illustrated by abnormal vascular
networks on conventional angiography or more than two flow voids
in the basal ganglia on MRI

Findings 1 and 2 are present bilaterally

Known diseases with similar angiographic findings (i.e., arteriosclerosis, autoimmune disease,
meningitis, brain neoplasm, Down syndrome, neurofibromatosis type 1,
head trauma, irradiation to the head, protein C deficiency, protein S deficiency,
and other diseases) should be ruled out

Broad classification: any steno-occlusive lesions that fulfill the following findings:

Steno-occlusive lesions around the terminal portions of the internal carotid arteries

Findings of moyamoya vessels may be absent

Bilateral involvement is not essential

Known diseases with similar angiographic findings should be ruled out

RCMJ, Research Committee on Moyamoya Disease of the Ministry of Health, Welfare and Labor, Japan in 1997; MRI, magnetic resonance imaging
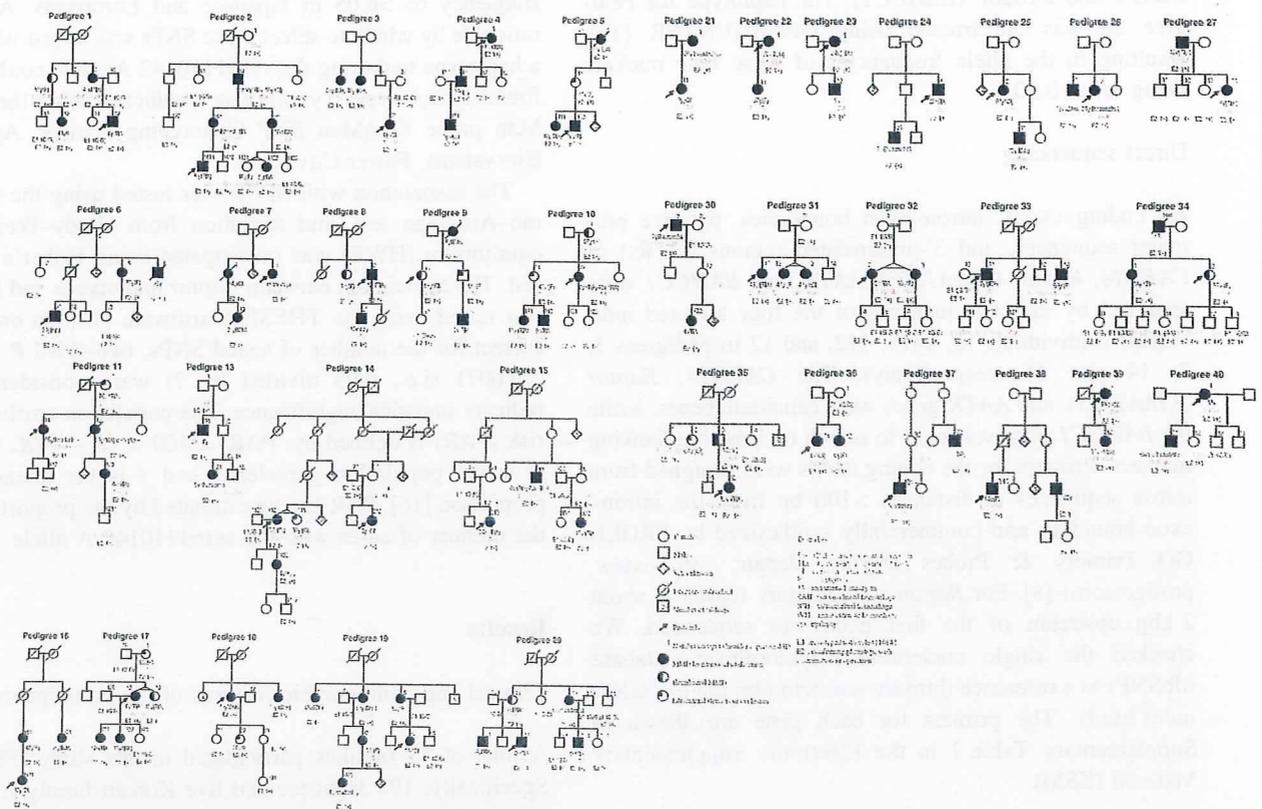
Fig. 1 Segregation of the ss161110142 A allele in *Raptor* in patients with the Moyamoya disease (MMD) phenotype. All affected individuals tested showed complete segregation for the 34 pedigrees.

Genomic DNA samples were not available for pedigrees 4, 5, and 18 and for individuals 1122 and 11222 of pedigree 14

rs2292971) were genotyped at 5.1-Mb intervals in the 17q25-qter linkage region [8]. The marker locations were obtained from NCBI Map Viewer (http://www.ncbi.nlm.nih.gov/mapview/). The linkage analysis was performed using a multipoint parametric linkage method, assuming a dominant model [7, 8]. We assumed that obligatory carriers should be treated as affected, as previously reported [8]. The phenotype of unaffected related individuals in the

pedigrees was classified as "unknown", while "non-founder" spouses were classified as "unaffected". On the basis of the observed prevalence of 6.03 per 100,000 persons [10], the disease allele frequency should be set at 0.00003015, but we set it more conservatively at 0.0001 owing to the increasing number of asymptomatic patients that have recently been diagnosed by magnetic resonance imaging (MRI) and MRA [11]. We therefore assumed a phenocopy frequency of 0.00001. The allele frequencies for each microsatellite marker were estimated from all unrelated founders using the Merlin software [12]. Analyses were carried out using GENEHUNTER ver. 2.0 (http://www.broad.mit.edu/ftp/distribution/software/genehunter/) [13].

Since individual 132 of Pedigree 20 had recombination between rs2280147 and rs2293099, we determined the 3′ flanking region by further additional markers, namely rs71166116 (*CHMP6*), rs9896314 (*AZI1*), rs62075318 (*AZI1*), and P1026P (*BAHCC1*). The haplotype for Pedigree 20 was constructed using GENEHUNTER [13], resulting in the allele frequencies of these four markers being set at 0.50.

Direct sequencing

All coding exons, intron–exon boundaries, putative promoter sequences, and 3′-untranslated regions (UTRs) of *CARD14*, *Raptor* (*KIAA1303*), *AATK*, and *BAHCC1* were analyzed by direct sequencing of the four affected individuals (individuals 12, 1411, 112, and 12 in pedigrees 1, 2, 14 and 15, respectively). The *CARD14*, *Raptor* (*KIAA1303*), and *AATK* genes were candidate genes, while the *BAHCC1* gene was used to search for possible flanking markers. Primers for the coding exons were designed from intron sequences at distances >100 bp from the intron–exon boundary and commercially synthesized by PROLIGO Primers & Probes (Kyoto, Japan; http://www.proligo.com) [8]. For *Raptor*, a regulatory region at about 2 kbp upstream of the first exon was sequenced. We checked the single nucleotide polymorphism database (dbSNP) as a reference (http://www.ncbi.nlm.nih.gov/SNP/index.html). The primers for each gene are shown in Supplementary Table 1 in the Electronic Supplementary Material (ESM).

Confirmation of segregation and linkage in familial cases

A variant (ss161110142) located at position −1480 from the transcription site of the *Raptor* gene was tested for segregation and linkage in the entire families. For three of the 37 families (pedigrees 4, 5, and 18, respectively), we were unable to test the segregation and linkage owing to the lack of availability of current DNA samples (Fig. 1).

In pedigree 14, genomic DNA samples were not available for individuals 1122 and 11222. The two-point logarithm of the odds ratio (LOD) score was calculated for the 34 genotyped pedigrees using GENHUNTER with the same parameter set as that used for the mapping described above. The penetrance was estimated as the proportion of subjects with MMD according to the broad classification among the genotyped subjects with the A allele of the ss161110142 G/A SNP.

Association study and statistical analysis

Six other *Raptor* SNPs, namely, rs9911978, rs12950635, rs4890047, rs4889863, rs11655474, and rs8080957, were then tested for association with MMD in the case–control study. These SNPs were selected to capture the variability of the first 65 kb of the *Raptor* gene by using the Tagger program [14] with criteria of $r^2 > 0.65$ and a minor allele frequency of >0.05 in Japanese and Europeans. A third rationale by which to select these SNPs was to test whether a haplotype harboring the ss161110142 A allele could be a founder haplotype. Typing was conducted using the Taq-Man probe (TaqMan SNP Genotyping Assays; Applied Biosystems, Foster City, CA).

The association with MMD was tested using the Cochran–Armitage test, and deviation from Hardy–Weinberg equilibrium (HWE) was investigated using Fisher's exact test. The association between *Raptor* haplotypes and MMD was tested using the THESIAS software [15]. In order to correct for the number of tested SNPs, two-sided P values <0.0071 (i.e., 0.05 divided by 7) were considered to indicate statistical significance. The population attributable risk (PAR) is defined by: $PAR = 100 \times (K - y)/K$, where K is the population prevalence and y is the phenocopy proportion [16]. PAR can be estimated by the proportion of the number of cases with the ss161110142 A allele.

Results

Clinical and demographic features of the participants

A total of 37 families participated in this study (Fig. 1). Specifically, 194 Japanese and five Korean family participants joined the study (Table 2). There were three peaks for clinical onset among Japanese patients: the first peak occurred at <10 years of age, the second small peak at 30–40 years, and the third peak at 50–60 years. Approximately, 42% of the Japanese patients were diagnosed before the age of 15 years. Thee major symptom of these pediatric patients was transient ischemic attacks (TIA). In contrast, the absence of symptoms or hemorrhage were the major symptoms in adult cases. These observations are consistent with a recent nationwide study [10].

Table 2 Summary of demographic and clinical profiles of cases and controls

Study cohort	Familial participant		Single subject participant			
Cases	Japanese	Korean	Japanese	Korean	Chinese	Caucasian
Number of participants	194	5	90	41	23	25
Age (mean ± SD)	39.2 ± 20.6	23.1 ± 12.8	47.7 ± 18.8	38.3 ± 13.4	25.3 ± 13.3	26.4 ± 15.2
Female:male	119:75	3:2	68:22	28:13	14:9	17:8
Number of pedigrees	36	1	0	–	0	0
Number of patients	109	2	–	–	–	–
Female:male	76:33	1:1	–	–	–	–
Family history	–	–	0	3	0	0
Characterization of patients						
Age of onset (years)						
<10	29	1	19	0	7	14
10–20	17	0	8	5	6	0
20–30	11	0	7	7	4	3
30–40	16	1	9	9	3	5
40–50	9	0	25	12	3	2
50–60	16	0	10	5	0	1
60+	11	0	8	3	0	0
Unknown	0	0	4	0	0	0
Young onset (<15)	46	1	25	1	10	14
Adult onset (15≤)	63	1	61	40	13	11
Clinical symptoms						
Cerebral infarction	13	0	8	14	3	11
TIA	39	1	33	8	1	2
Hemorrhage	14	0	19	0	3	1
Unknown stroke	1	1	1	16	6	3
Seizure	5	0	1	0	0	2
Headache	9	0	8	2	2	3
Asymptomatic	23	0	4	0	0	1
Other	5	0	16	1	8	2
Total	109	2	90	41	23	25
Clinical symptoms: young onset (<15 years)						
Cerebral infarction	4	0	0	0	1	2
TIA	29	1	16	0	1	2
Hemorrhage	0	0	2	0	0	0
Unknown stroke	1	0	0	1	2	3
Seizure	4	0	0	0	0	2
Headache	4	0	5	0	0	3
Asymptomatic	2	0	0	0	0	1
Other	2	0	2	0	6	1
Total	46	1	25	1	10	14
Female:male	28:18	0:1	22:3	1:0	6:4	9:5
Clinical symptoms: adult onset (≥15 years)						
Cerebral infarction	9	0	8	14	2	9
TIA	10	0	17	8	0	0
Hemorrhage	14	0	17	0	3	1
Unknown stroke	0	1	1	15	4	0
Seizure	1	0	1	0	0	0
Headache	5	0	3	2	2	0

Table 2 continued

Study cohort	Familial participant		Single subject participant			
Cases	Japanese	Korean	Japanese	Korean	Chinese	Caucasian
Asymptomatic	21	0	4	0	0	0
Other	3	0	10	1	2	1
Total	63	1	61	40	13	11
Female:male	48:15	1:0	43:18	27:13	8:5	8:3

Controls	Japanese	Korean	Chinese	Caucasian
Number of participants	384	223	100	164
Age (mean ± SD)	60.8 ± 9.6	40.0 ± 8.4	38.2 ± 10.3	48.0 ± 19.6
Female:male	205:179	198:25	100:0	71:93
Angiography[a]	384	46	0	68
Screening by angiography (%)	100.0	20.6	0	41.5

TIA, Transient ischemic attack; other, including unknown symptoms or other types; SD, standard deviation

[a] Angiography: conventional angiography, magnetic resonance angiography (MRA), computed tomography (CT), among others

The study also included 90 Japanese, 41 Korean, 23 Chinese, and 25 Caucasian singular participants (Table 2). With the exception of three cases, none of these patients had family histories.

A brief description of the 384 Japanese, 223 Korean, 100 Chinese, and 164 Caucasian controls is given in Table 2.

Fine mapping of the 17q25.3

The addition of the two newly recruited families (pedigrees 19 and 20) increased the LOD score from 8.07 [8] to 9.67. One patient (individual 132 in pedigree 20) had recombination between rs2280147 and rs2293099 (Supplementary Fig. 1 in ESM). Fine mapping using the four additional SNPs, namely, rs71166116 (CHMP6), rs9896314 (AZI1), rs62075318 (AZI1), and P1026P (C>T) (BAHCC1), revealed recombination between rs62075318 and a variant in BAHCC1 (P1026P) in pedigree 20, indicating that the core region was a 2.1-Mb region between D17S1806 and BAHCC1 (P1026P).

This region contained 40 genes, including BAIAP2, whose sequence was reported in our earlier publication [8]. To select candidate genes, we chose the key words "inflammation" [17], "apoptosis" [18] or "proliferation" and "vascular system" [3, 4], all of which have been reported to be associated with pathological conditions of MMD. The selected genes were CARD14, which plays key roles in immune reactions [19], AATK, which is reported to be involved in apoptosis [20], and Raptor [regulatory associated protein of mammalian target of rapamycin (mTOR)] [21], which is associated with tissue hypertrophy

[22], is a regulator of hypoxia-inducible factor [23], and is involved in HLA class I antibody-mediated endothelial cell proliferation [24].

Sequencing

We sequenced CARD14, Raptor, and AATK in four unrelated affected individuals. The results are shown in Supplementary Table 2 in ESM. Among these SNPs, the Raptor ss161110142 G/A polymorphism appeared to be very interesting because all four sequenced affected individuals were found to be heterozygous.

Confirmation of segregation and linkage with the ss161110142

We then genotyped the 34 families for the ss161110142 G/A SNP. As shown in Fig. 1, all affected individuals in the tested families were found to carry the ss161110142 A allele and showed complete segregation. The two-point LOD score was calculated to be 14.2 ($P = 3.89 \times 10^{-8}$). The estimated penetrance of the A allele was 74.0% (88/119) [95% confidence interval (CI) 66–82%].

Association study

The last stage of our analysis consisted of a case–control association study for MMD performed in different ethnicities. The ss161110142 A allele was common in the Asian cases (from 4% in Chinese cases to 33% in Korean cases), while its frequency was about 1% in Japanese and Korean controls (Table 3). The ss161110142 A allele was not

Table 3 Association between seven SNPs in *Raptor* and Moyamoya disease among the different populations

rs ID[a]	Allele 1/2	Populations	Controls					Cases					OR[d] (95% CI)	P[e]
			11	12	22	Frequency[b]	P, HWE[c]	11	12	22	Frequency[b]	P, HWE[c]		
ss161110142	G/A	Japanese	377 98.18%	6 1.56%	1 0.26%	0.01	0.072	46 51.11%	42 46.67%	2 2.22%	0.26	0.056	51.52 (21.92–121.05)	2.08×10^{-29}
		Korean	218 97.76%	5 2.24%	0 0.00%	0.01	1.000	14 34.15%	27 65.85%	0 0.00%	0.33	0.003	84.09 (28.08–251.76)	9.42×10^{-22}
		Chinese	100 100.00%	0 0.00%	0 0.00%	0.00	1.000	21 91.30%	2 8.70%	0 0.00%	0.04	1.000	NA	3.37×10^{-2}
		All Asian	695 98.30%	11 1.56%	1 0.14%	0.01	0.108	81 52.60%	71 46.10%	2 1.30%	0.24	0.002	52.20 (27.18–100.23)	2.48×10^{-49}
		Caucasian	164 100.00%	0 0.00%	0 0.00%	0.00	1.000	25 100.00%	0 0.00%	0 0.00%	0.00	1.000	NA	NA
rs9911978	A/G	Japanese	149 38.80%	177 46.09%	58 15.10%	0.38	0.707	16 17.78%	53 58.89%	21 23.33%	0.53	0.144	1.81 (1.31–2.51)	3.00×10^{-4}
		Korean	82 36.77%	101 45.29%	40 17.94%	0.41	0.421	8 19.51%	21 51.22%	12 29.27%	0.55	1.000	1.78 (1.11–2.86)	0.016
		Chinese	29 29.00%	51 51.00%	20 20.00%	0.46	0.975	10 43.48%	13 56.52%	0 0.00%	0.28	0.184	0.47 (0.23–0.95)	0.033
		All Asian	260 36.78%	329 46.53%	118 16.69%	0.40	0.457	34 22.08%	87 56.49%	33 21.43%	0.50	0.158	1.48 (1.16–1.90)	1.70×10^{-3}
		Caucasian	88 53.66%	61 37.20%	15 9.15%	0.28	0.437	13 52.00%	8 32.00%	4 16.00%	0.32	0.326	1.23 (0.65–2.33)	0.534
rs12950635	T/C	Japanese	48 12.50%	164 42.71%	172 44.79%	0.66	0.411	5 5.56%	40 44.44%	45 50.00%	0.72	0.484	1.33 (0.93–1.91)	0.118
		Korean	25 11.21%	82 36.77%	116 52.02%	0.70	0.105	5 12.20%	12 29.27%	24 58.54%	0.73	0.189	1.15 (0.68–1.95)	0.612
		Chinese	6 6.00%	34 34.00%	60 60.00%	0.77	0.844	3 13.04%	10 43.48%	10 43.48%	0.65	1.000	0.56 (0.28–1.12)	0.097
		All Asian	79 11.17%	280 39.60%	348 49.22%	0.69	0.059	13 8.44%	62 40.26%	79 51.30%	0.71	0.980	1.12 (0.85–1.47)	0.406
		Caucasian	4 2.44%	62 37.80%	98 59.76%	0.79	0.169	1 4.00%	10 40.00%	14 56.00%	0.76	1.000	0.86 (0.43–1.73)	0.671